

## Effect of alumina on ceramic properties of cordierite glass–ceramic from basalt rock

Salwa A.M. Abdel-Hameed<sup>a</sup>, I.M. Bakr<sup>b,\*</sup>

<sup>a</sup> Glass Research Department, National Research Center, P. Code 12622, Dokki, Cairo, Egypt

<sup>b</sup> Faculty of Engineering, Mattaria, Helwan University, Egypt

### Abstract

Cordierite–anorthite–alumina compositions have been obtained by mixing alumina powder with cordierite–anorthite glass powder which were previously prepared from basalt rock. Alumina has been added in progressive proportions ranging from 10 to 30%. The prepared specimens were thermally treated at 1100 °C for 3 h. Addition of alumina did not result in a new phase formation, but inhibits the cordierite grain growth. Adding 10% alumina had increased the porosity and decreased the modulus of rupture (MOR), but higher addition had not revealed an observable effect. Alumina content is observed to help in decreasing the dielectric constant.

© 2006 Published by Elsevier Ltd.

**Keywords:** Glass ceramics; Grain size; Mechanical properties; Thermal expansion; Cordierite

### 1. Introduction

Minerals that are capable of wide isomorphous substitutions and possess a good desired properties (e.g. cordierite and plagioclase) may be the basis for preparing useful glass–ceramics characterized by a wide spectrum of properties. From a technological standpoint plagioclase feldspar-based glass–ceramics exhibit high refractoriness and moderate coefficients of thermal expansion ( $\sim 35 \times 10^{-7} \text{ }^{\circ}\text{C}^{-1}$ ; 20–300 °C). Such glass–ceramic bodies, wherein the predominant crystal phase is anorthite ( $\text{CaAl}_2\text{Si}_2\text{O}_8$ ) or anorthite ss would have low dielectric constants and dc volume resistivities coupled with low ac dielectric losses, and consequently; would be competitive with commercial electrically conducting materials.<sup>1</sup> Also, glass–ceramics that include cordierite ( $2\text{MgO} \cdot 2\text{Al}_2\text{O}_3 \cdot 5\text{SiO}_2$ ) as a major crystalline phase are very strong and of much importance. They have excellent dielectric properties, good thermal stability and shock resistance, high deformation temperature, high chemical durability, high mechanical strength and low coefficient of expansion ( $\sim 10\text{--}22 \times 10^{-7} \text{ }^{\circ}\text{C}^{-1}$ ; 25–800 °C).<sup>2</sup> The list of industrial and commercial applications of cordierite-based glass–ceramics is extensive especially as insulators in spark plug and for the fabrication of integrated circuit devices in the silicon semiconductor

industry as it has a similar expansion to silicon and high volume resistivity.<sup>3–5</sup> A combination of two of said phases may thus result in a wider-range of glass–ceramic properties used in a wide range of applications such as supports of catalysts for the conversion of combustion gases from engines and industrial heat exchangers for gas turbines.<sup>6</sup>

In spite of cordierite composition varies between the limits expressed by the formulas  $2\text{MgO} \cdot 2\text{Al}_2\text{O}_3 \cdot 5\text{SiO}_2$  and  $\text{MgO} \cdot \text{Al}_2\text{O}_3 \cdot 3\text{SiO}_2$ , samples in this range tend to show abrupt maturation processes and their production is difficult to control.<sup>7</sup> As far as the authors are aware, crystallization of such vitreous cordierite phase from basaltic rock, which greatly deviated from its stoichiometry, have yet not been published.

Many studies on glass ceramic composites involving model systems, e.g.  $\text{ThO}_2$ ,  $\text{Al}_2\text{O}_3$ , and  $\text{ZrO}_2$  dispersions in a glass matrix have been previously followed. The strength of the composite increases with smaller particle size and higher volume fraction of the dispersed particles.<sup>8</sup>

Alumina is expected to be a good reinforcement material for cordierite–anorthite glass ceramics due to its excellent mechanical properties.

To formulate cordierite–anorthite glass–ceramic batch composition, a chemico-mineral molecular norm (CIPW)<sup>9</sup> was adopted to recalculate the chemical composition of basalt into cordierite and anorthite molecules. In this method of calculation, and to achieve the highest possible amount of cordierite from such polycomponents basalt composition;

\* Corresponding author. Fax: +20 2 337 0931.

E-mail address: [agmothman@yalla.com](mailto:agmothman@yalla.com) (I.M. Bakr).

Table 1

Calculated chemical composition (in wt.%) of the investigated basaltic cordierite–anorthite glasses

Oxide	Wt.%
SiO <sub>2</sub>	42.01
Al <sub>2</sub> O <sub>3</sub>	26.48
TiO <sub>2</sub>	10.09
FeO	6.38
CaO	6.29
MgO	3.58
Na <sub>2</sub> O	1.44
K <sub>2</sub> O	0.43
LiF	1.50
MgF <sub>2</sub>	1.80

addition of deliberately calculated amount of (i) a reducing agent (e.g. sucrose) was added to convert Fe<sup>3+</sup> present in basalt to Fe<sup>2+</sup>; since the capability of the latter to be isomorphously shared in the cordierite structure is much more than Fe<sup>3+</sup>; (ii) TiO<sub>2</sub> which has a significant reducing effect on the melting temperature and viscosity of cordieritic glass compositions; (iii) kaolin to compensate the deficiency of Al<sub>2</sub>O<sub>3</sub> in basalt and consequently satisfying the cordierite ss formation; (iv) F<sup>−</sup> in the form of Li and Mg fluoride as nucleating agent.

The main purpose of the present paper is to study the effect of  $\alpha$ -Al<sub>2</sub>O<sub>3</sub> additions on the crystallization sequence, thermal, physical, mechanical and electrical properties of cordieritic glass ceramics from modified basalt-based glasses.

## 2. Experimental

The starting glass compositions (Table 1) from basalt rock as a main reagent with minor amount of kaolin, TiO<sub>2</sub>, LiF and MgF<sub>2</sub> were melted well at 1450 °C for 3 h in a platinum crucibles yielding homogeneous blackish seed-free glasses with good workability traits. The melt was then cast into hot steel moulds in the form of discs and rods which were transferred to a muffle furnace at 650 °C for annealing. Glass fragments were grounded using agait mortar to grain size  $\sim 63 \mu\text{m}$ .

Alumina was added to the cordierite–anorthite glass powder in different proportions resulting in four batches as given in Table 2. Alumina has a mean particle size of 5.5  $\mu\text{m}$ . Powders were mixed thoroughly, then uni-axial pressed in a steel die to a 12 mm diameter discs at 150 MPa. Also rods of dimensions 70 mm  $\times$  10 mm  $\times$  10 mm were pressed at the same pressure in order to measure the bending strength. Pressed specimens were fired in an electric furnace at 1100 °C for 3 h soaking time. This firing temperature was selected according to

Table 2

Prepared cordierite–anorthite–alumina composite batches

Batch symbol	Alumina (%)	Glass (%)
C <sub>0</sub>	0	100
C <sub>10</sub>	10	90
C <sub>20</sub>	20	80
C <sub>30</sub>	30	70

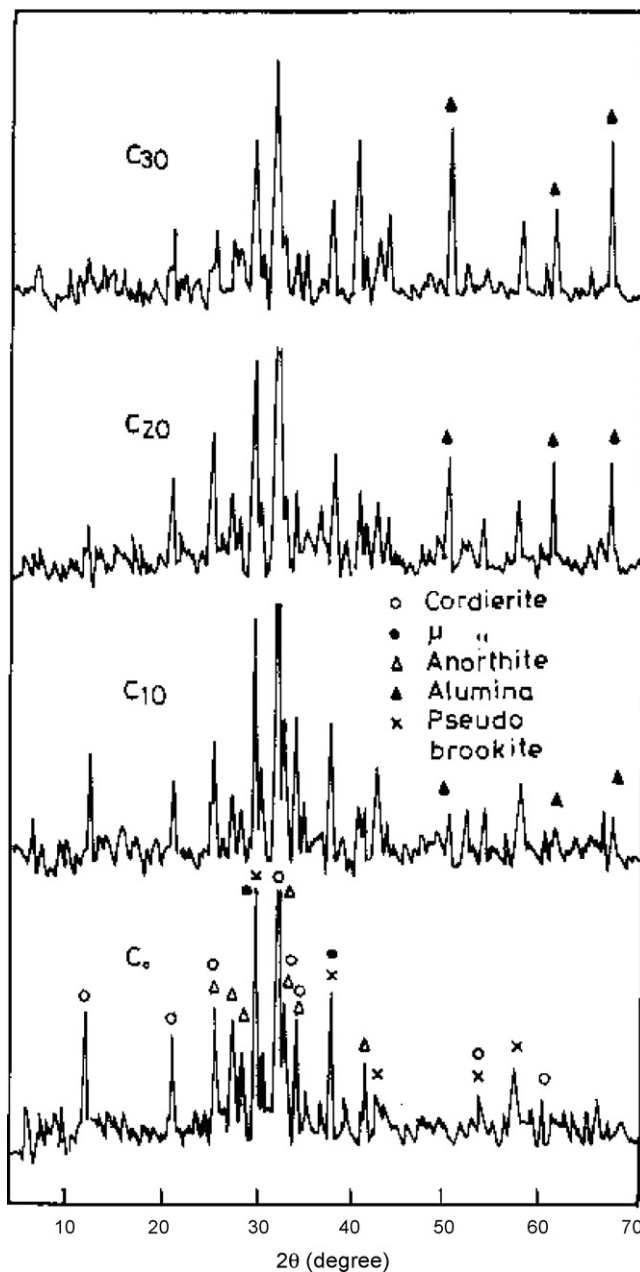


Fig. 1. XRD of C<sub>0</sub>, C<sub>10</sub>, C<sub>20</sub> and C<sub>30</sub> heat-treated at 1100 °C/3 h.

the previously known crystallization temperature of cordierite–anorthite.<sup>9</sup>

Identification of crystalline phases was carried out by X-ray diffraction using a diffractometer type Bruker D8 Advance, through the examination of fine powder of the samples by Cu K $\alpha$  radiation after thermal heat treatments. Fired specimens were polished, etched by 5% HF for 10 s, and gold coated, in order to be examined by Scanning electron microscopy (SEM: Jeol-840 A Electron Probe Microanalyzer).

Physical properties in terms of apparent porosity and bulk density were measured using Archimedes method. Bending strength of the fired specimens was determined using three points bend test. Thermal expansion coefficient was measured using Linseis L74/1250 dilatometer.

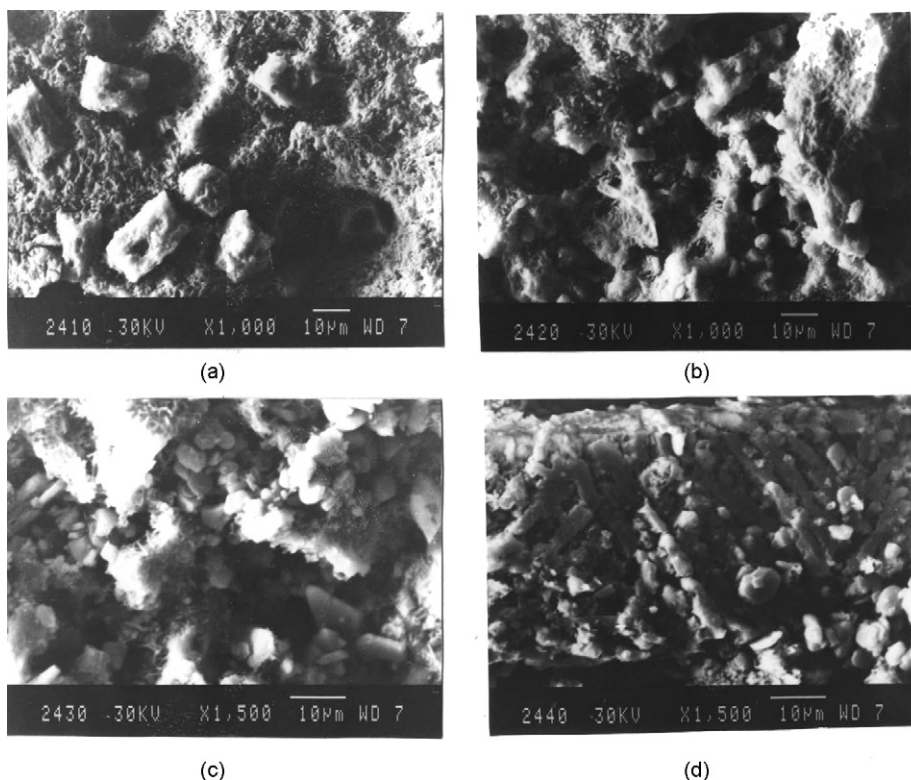


Fig. 2. SEM of  $C_0$ ,  $C_{10}$ ,  $C_{20}$  and  $C_{30}$  heat-treated at  $1100^\circ\text{C}/3\text{ h}$ .

### 3. Results and discussion

As shown in Fig. 1, the isothermal treatment of the base composition ( $C_0$ ) at  $1100^\circ\text{C}$ , and 3 h results in the crystallization of  $\alpha$ -cordierite, anorthite,  $\beta$ -quartz ss ( $\mu$ -cordierite) as major phases, as well as pseudobrookite as minor phase. X-ray analysis of samples  $C_{10}$ ,  $C_{20}$  and  $C_{30}$  reveals the appearance of  $\alpha$ - $\text{Al}_2\text{O}_3$  in addition to the previously detected phases in  $C_0$ . The peaks intensity of  $\alpha$ - $\text{Al}_2\text{O}_3$  increases from  $C_{10}$  to  $C_{30}$  on the expense of intensities of other phases which decrease greatly from  $C_0$  to  $C_{30}$ . No other new phases were observed with alumina additions. This is referred to the absence of any reaction at these conditions.

SEM of base sample  $C_0$  heat-treated at  $1100^\circ\text{C}/3\text{ h}$  shows crystallization of well developed hexagonal cordierite embedded in anorthite fibers (Fig. 2a). Adding 10%  $\text{Al}_2\text{O}_3$  results in the appearance of some  $\text{Al}_2\text{O}_3$  rods in addition to cordierite and anorthite fibers (Fig. 2b). Higher additions of  $\text{Al}_2\text{O}_3$  leads to increase the amount of  $\text{Al}_2\text{O}_3$  rods on the expense of anorthite fibers (Fig. 2c). Sample  $C_{30}$  shows many aggregates of  $\text{Al}_2\text{O}_3$  beside anorthite and cordierite crystals (Fig. 2d). From the above figures it is noticed that increasing the amount of  $\text{Al}_2\text{O}_3$  leads to inhibit the grain growth of cordierite crystals and amount of anorthite fibers. The above observation may be due to increase the viscosity of the glassy matrix by adding  $\text{Al}_2\text{O}_3$  which resulted in low migration of ions leading to small crystal growth of both cordierite and anorthite (compare Fig. 2a and d).

Fig. 3 represents the variation of apparent porosity and bulk density with the addition of alumina. It is clear that the specimen prepared from cordieritic glass only has the highest bulk

density ( $2.55\text{ g/cm}^3$ ) and lowest porosity (2.17%). Addition of 10% alumina causes a sharp increase of porosity (24.0%) and a considerable decrease of bulk density (2.16). Further additions of alumina up to 30% results only in a small increase of the porosity and approximately no change in bulk density. The sudden increase of the porosity at 10% alumina content may be referred to the great difference of thermal expansion between alumina ( $8.8 \times 10^{-6}^\circ\text{C}^{-1}$ )<sup>10</sup> and cordierite–anorthite glass. That means alumina particles contracts on cooling leaving surrounding pores. The lack of sinterability can also be explained by the Scherer models, according to which, rigid and incompressible inclusions retard the densification of bodies by creating a circumferential tensile stress in the matrix phase.<sup>11</sup>

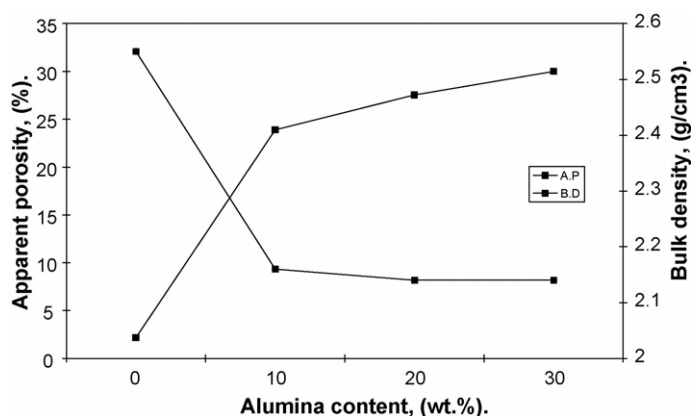


Fig. 3. Effect of alumina content on the apparent porosity and bulk density of the studied specimens.

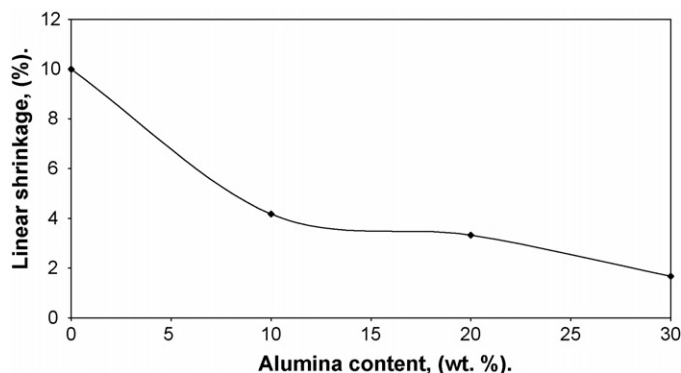


Fig. 4. Effect of alumina content on the linear shrinkage of the studied specimens.

While increasing the alumina content over than 10% seems to suppress the pores propagation inside the matrix. That is why no abrupt porosity change occurred with higher additions of alumina. Bulk density decreased largely in sample C<sub>10</sub> compared to sample C<sub>0</sub> due to the great increase of porosity. Although the apparent porosity decreased in a small extent from sample C<sub>10</sub> to sample C<sub>30</sub>, no detectable change occurred in the bulk density of these samples. This is due to the high density of alumina which compensate the decrease of density caused by higher pores.

Fig. 4 represents the change of linear shrinkage with alumina content. The linear shrinkage decreased largely from sample C<sub>0</sub> to C<sub>10</sub> and then decreased smoothly from C<sub>10</sub> to C<sub>30</sub>. This pattern is compatible with the change of porosity. The high porosity leads to a little shrinkage.

The expansion coefficient of samples C<sub>0</sub> and C<sub>30</sub> shows in general moderate thermal expansion coefficient till 700 °C. It is noticed that C<sub>30</sub> revealed slight increase in  $\alpha$  compared to the base composition C<sub>0</sub>. The presence of cordierite which have low thermal expansion coefficient with anorthite which have relatively higher value of  $\alpha$  in C<sub>0</sub> results in moderate thermal expansion coefficient of the final product. Although Al<sub>2</sub>O<sub>3</sub> have high thermal expansion coefficient, the cordierite–anorthite–Al<sub>2</sub>O<sub>3</sub> composite (C<sub>30</sub>) has slightly higher  $\alpha$  than C<sub>0</sub>. This is attributed to the partial replacement of anorthite by Al<sub>2</sub>O<sub>3</sub> which have near value of  $\alpha$  (Table 3).

The dielectric constant of the fired composites was measured at 100 kHz. The samples were prepared in the form of discs of 10 mm in diameter and 1 mm thickness by cutting of the sintered bodies. Philips R.L.C. bridge type PM 6304 programmable automatic RLC meter was used for measuring the dielectric constant ( $\epsilon$ ) at room temperature. To enable high-speed switching of large-scale integrators (LSIs) in a system, the circuit boards should have a low dielectric constant, thus following the high-speed signal to propagate with a shorter delay.<sup>12,13</sup>

Table 3  
Thermal expansion coefficient  $\alpha$  ( $\times 10^{-6} \text{ } ^\circ\text{C}^{-1}$ ) of sample heat treated at 1100 °C/3 h

Sample	300 °C	400 °C	500 °C	600 °C	700 °C
C <sub>0</sub>	5.3	5.4	5.4	5.6	–
C <sub>30</sub>	5.4	5.5	5.7	5.8	6.0

Table 4

Dielectric constant ( $\epsilon$ ) and phases developed of different composites sintered at 1100 °C/3 h at 100 kHz

Sample	Dielectric constant ( $\epsilon$ )	Phases developed
C <sub>0</sub>	10.3	$\alpha$ -Cordierite, anorthite, $\beta$ -quartz ss and pseudobrookite
C <sub>10</sub>	8.9	$\alpha$ -Cordierite, anorthite, $\beta$ -quartz ss and pseudobrookite + $\alpha$ -Al <sub>2</sub> O <sub>3</sub>
C <sub>20</sub>	8.8	$\alpha$ -Cordierite, anorthite, $\beta$ -quartz ss and pseudobrookite + $\alpha$ -Al <sub>2</sub> O <sub>3</sub>
C <sub>30</sub>	8.3	$\alpha$ -Cordierite, anorthite, $\beta$ -quartz ss and pseudobrookite + $\alpha$ -Al <sub>2</sub> O <sub>3</sub>

Table 5

Modulus of rupture of the studied batches (MPa)

Sample	MOR
C <sub>0</sub>	67
C <sub>10</sub>	51.5
C <sub>20</sub>	52
C <sub>30</sub>	52

It is noticed that the dielectric constant in general is low and decreases with the increase of alumina content as shown in Table 4.

The mechanical features of the studied specimens are measured in terms of modulus of rupture, which are given in Table 5. The modulus of rupture decreased from 67 MPa for C<sub>0</sub> to 51.5 MPa for C<sub>10</sub> and remained constant for the other specimens. The decrease of modulus of rupture at first is referred to the large increase of porosity. Although alumina has a higher modulus of rupture than cordierite, the high porosity of sample seems to play the main role in decreasing its modulus of rupture. The effect of alumina is obvious in samples C<sub>20</sub> and C<sub>30</sub> where the modulus of rupture remained constant in spite of the increase of porosity.

#### 4. Conclusion

1. Heat treatment of cordierite–anorthite glass powder prepared from basalt rock at 1100 °C, for 3 h resulted in the crystallization of well developed hexagonal cordierite, anorthite fibers,  $\beta$ -quartz and a little portion of pseudobrookite.
2. Addition of alumina in the range from 10 to 30% did not result in any reaction with the other glass constituents, since no new phases were detected.
3. Additions of 10 and 20% alumina caused an inhibition for the grain growth of cordierite crystals, which is advantageous from the mechanical stand point of view.
4. A sudden increase of the apparent porosity was observed at 10% alumina due to the mismatch between the thermal expansion coefficients of alumina and cordierite–anorthite glass, while higher additions of alumina did not cause a remarkable increase of porosity.
5. Both of the base body and the specimen with 30% alumina have approximately the same value of thermal expansion coefficient.

6. Alumina additions gave the benefit of decreasing the dielectric constant.
7. Modulus of rupture decreased at 10% alumina content, but remained constant at higher alumina contents.

## References

1. Reade, R. F., US Patent 4,187,115, February 5, 1980.
2. Morell, R., The mineralogy and properties of sintered cordierite glass–ceramics. *Proc. Br. Ceram. Soc.*, 1979, **28**, 53–71.
3. McMillan, P. W., *Glass–Ceramics*, 2nd ed., London, 1979.
4. Strand, Z., Glass–ceramic materials. *Glass Science Technology*, Vol. 8. Elsevier Sci. Publ., 1985.
5. Watanabe, K. and Giess, E. A., Crystallization kinetics of high-cordierite glass. *J. Non-Cryst. Solids*, 1994, **169**, 306–310.
6. Boudchicha, M. R., Achour, S. and Harabi, A., Crystallization and sintering of cordierite and anorthite based binary ceramics. *J. Mater. Sci. Lett.*, 2001, **20**, 215–217.
7. Barry, T. I., Cox, J. M. and Morell, R., Cordierite glass–ceramics—effect of  $\text{TiO}_2$  and  $\text{ZrO}_2$  content on phase sequence during heat treatment. *J. Mater. Sci.*, 1978, **13**(3), 594–610.
8. Mussler, B. H. and Shafer, M. W., Preparation and properties of mullite–cordierite composites. *J. Am. Ceram. Soc. Bull.*, 1984, **63**(5), 705–714.
9. Abdel-Hameed, S. A. M., Effect of nucleation catalysts on crystallization of different modified basaltic glass–ceramic compositions. Ph.D. Ain Shams Univ., Egypt, 1999.
10. Kingery, W. D., Bowen, H. K. and Uhlman, D. R., *Introduction to Ceramics* (2nd ed.). John Wiley and Sons, New York, 1975.
11. Yekta, B. E. and Marghussian, V. K., Sintering of  $\beta$ -quartz ss and gahnite glass–ceramic/silicon carbide composites. *J. Eur. Ceram. Soc.*, 1999, **19**, 2969–2973.
12. Schwartz, B., Review of multiplayer ceramics for microelectronic packaging. *J. Phys. Chem. Solids*, 1984, **45**(10), 1051–1068.
13. Bodgett Jr., A. J., Multi-chip module. In *Proceeding of the 30th Electronic Components Conference*, Vol. 30, 1980, pp. 283–285.